Raman scattering studies of composites based on Cu_6PS_5X (X = I, Br) superionic nanocrystals

I.P. Studenyak[1], M. Kranjčec[2], R.Yu. Buchuk[1], V.O. Stephanovich[1], S. Kökényesi[3]
[1]*Uzhhorod National University, Physics Faculty,*
46, Pidhirna str. 88000 Uzhhorod, Ukraine
[2]*University of Zagreb, Geotechnical Faculty,*
Hallerova Aleja 7, 42000 Varaždin, Croatia
[3]*University of Debrecen, Institute of Physics,*
Bem tér 18/a, 4028 Debrecen, Hungary
E-mail:studenyak@dr.com

Abstract. Composites were prepared by mixing Cu_6PS_5X (X = I, Br) nanocrystalline powders obtained by ball milling with different polymers. The average nanocrystal size was estimated from X-ray diffraction; the composites were studied by scanning electron microscopy. Phonon spectra of nanocomposites with different polymer matrices, size and concentration of nanocrystals were studied using Raman spectroscopy. It has been revealed that the surface-to-bulk phonon integrated intensity ratio strongly varies with the type of polymer matrix, average grain size and concentration of nanocrystals.

Keywords: composite, nanocrystal, Raman scattering, surface phonon.

1. Introduction

Cu_6PS_5X (X = I, Br) crystals belong to the family of compounds with argyrodite structure and are characterized by high ionic conductivity [1-4]. The latter defines the possibilities of their practical application as solid electrolyte sources of energy, sensors and highly efficient capacitors. At room temperature, they belong to the cubic crystal system ($F\bar{4}3m$ space group), while below the room temperature they undergo two phase transitions [4, 5]. The phase transitions in Cu_6PS_5X (X = I, Br) crystals are accompanied by anomalous behaviour of dielectric, acoustic, calorimetric, and optical properties [3-9]. In few recent years, much attention was devoted to studies of composites and nanocrystalline powders based on Cu_6PS_5X (X = I, Br) superionic conductors [10 – 14].

Now it is important to obtain nanostructures based on argyrodite-structure superionic conductors, which would enable one to vary their physical properties and spheres of application. It is well known that, with size decrease from bulk to nanometric materials, the role of surface essentially increases due to increase of the surface-to-volume ratio. In spite of the fact that the

optical properties of bulk crystals of Cu_6PS_5X (X = I, Br) superionic conductors have been studied extensively enough, studies of their changes due to transfer to nanometric sizes begin just now. Therefore, the present work is aimed at the investigation of specific features in Raman scattering spectra of composites based on Cu_6PS_5X (X = I, Br) nanocrystals.

2. Experimental

Cu_6PS_5X (X = I, Br) single crystals were grown using chemical vapour transport [9]. High-purity Cu, P, S and copper monohalide obtained by precipitation from aqueous solutions and distilled in vacuum were used as initial components for the synthesis. The copper monohalide was used as the transport agent (10–20 mg per 1 cm^3 of the ampoule free volume). The single crystals were grown in the shape of reddish orange 5×5×2 mm-size plates or 4×4×4 mm-size distorted tetrahedra. The microcrystalline powders of various grain sizes were obtained by ball milling this material in a stainless steel cylindrical vial with hardened steel balls. The grain size reduction achieved during each milling step was followed by measuring the XRD spectra of the powders with a horizontal Siemens diffractometer by using Cu $K_{\alpha 1}$ radiation.

Composites based on the Cu_6PS_5X (X = I, Br) nanocrystalline powders were obtained by mixing them with solutions of the following polymers: (i) polyvinylchloride (PVC), (ii) polytrifluorethylene (PFE), (iii) copolymer of styrene with maleic anhydride (CSMA). Besides, in order to increase the composite plasticity and to activate the solution process as well as to obtain uniform distribution of nanoparticles, these mixtures were modified by introduction of plasticators (o-nitrophenyl octyl ester, dibutylphtalate) and stabilizing agents (e.g., trys-(hydroxymethyl) methylamine). The structure of the composites was studied by scanning electron microscopy (Hitachi S-4300), the corresponding data being presented in Fig. 1. It is shown that the nanocrystals are partly uniformly distributed in the polymer matrix and partly conglomerated in rather large units which are more than an order of magnitude higher than the average grain size.

Raman scattering measurements were performed using a LOMO DFS-24 double grating monochromator, the excitation being provided by a He–Ne laser (632.8 nm). The slit spectral width did not exceed 1 cm^{-1}.

## 3. Results and discussion

Raman scattering studies of composites based on Cu_6PS_5X (X = I, Br) nanocrystals were performed for samples with different polymer matrices, size and concentration of nanocrystals (Figs 2 and 3). It should be noted that in the Raman spectrum of the bulk crystals separate groups of bands are observed [4]. In the low-frequency range (below 100 cm^{-1}) the bands corresponding to diffusive-type vibrations of Cu atoms and $Cu - X$ bond vibrations are manifested. In the range near 315 cm^{-1} a broad asymmetric band is revealed, resulting from superposition of a doubly degenerate E mode and a triply degenerate F_2 mode. Within the frequency range 400 to 450 cm^{-1} in the Raman spectra, all the samples contain a band corresponding to A_1 symmetry vibrations which are the most pronounced in the spectra. Within the range 500 to 600 cm^{-1}, two bands were observed in the spectra. They are related to TO and LO vibrations of the F_2 mode corresponding to internal stretching vibrations of PS_4^{3-} tetrahedral groups [4].

It is shown in [13, 14] that for Cu_6PS_5X (X = I, Br) nanocrystalline powders a considerable increase of Rayleigh scattering, masking the low-frequency Raman bands, is observed. Hence, only the Raman bands above 100 cm^{-1} could be detected. The spectra of the nanocrystalline powders contain two distinct maxima, the higher frequency one corresponding to the A_1 symmetry vibration, and the lower frequency one being a superposition of E and F_2 symmetry modes. The crystal size reduction results in a low-frequency shift of both bands, their broadening and decrease in intensity. For Cu_6PS_5I nanocrystals, the spectral position of the A_1 band shifts from 420 down to 414 cm^{-1}, for Cu_6PS_5Br nanocrystals – from 425 down to 421 cm^{-1}, and their halfwidths increase from 3 up to 8 cm^{-1}. The maximum position of the band formed by E and F_2 symmetry vibrations in the case of Cu_6PS_5I nanocrystals shifts from 313 down to 303 cm^{-1}, and its halfwidth increases from 21 up to 33 cm^{-1}, while in the case of Cu_6PS_5Br it shifts from 315 down to 305 cm^{-1}, and its halfwidth increases from 20 up to 30 cm^{-1}. In both cases, the halfwidths were estimated after Rayleigh wing constituent having been subtracted. Finally, evolution of the Raman spectra of Cu_6PS_5X (X = I, Br) nanocrystalline powders occurring as a result of decreasing the nanocrystal size is explained predominantly by surface phonon modes, which contribution to the Raman spectrum increases due to the higher surface-to-volume ratio [13, 14].

In polymer composites based on Cu_6PS_5X (X = I, Br) nanocrystals as well as in micro- and nanopowders, an essential growth of the Rayleigh scattering is observed. In comparison with the Raman spectra of nanopowders, Raman spectra of the nanocomposites contain only the A_1 band, while the one formed by the superposition of E and F_2 symmetry modes, is either pronounced very weakly, or not revealed at all (Figs 2 and 3). It is shown that the decrease of the nanocrystal concentration leads to the intensity decrease of the above mentioned bands, while the decrease of the nanocrystal size additionally leads to the low-frequency shift of the band formed by the E and F_2 symmetry vibrations (Figs 2 and 3).
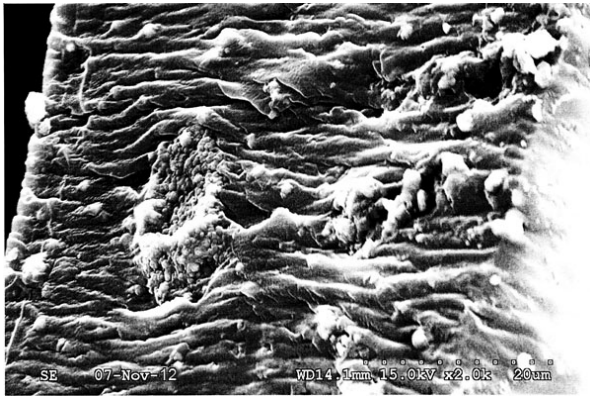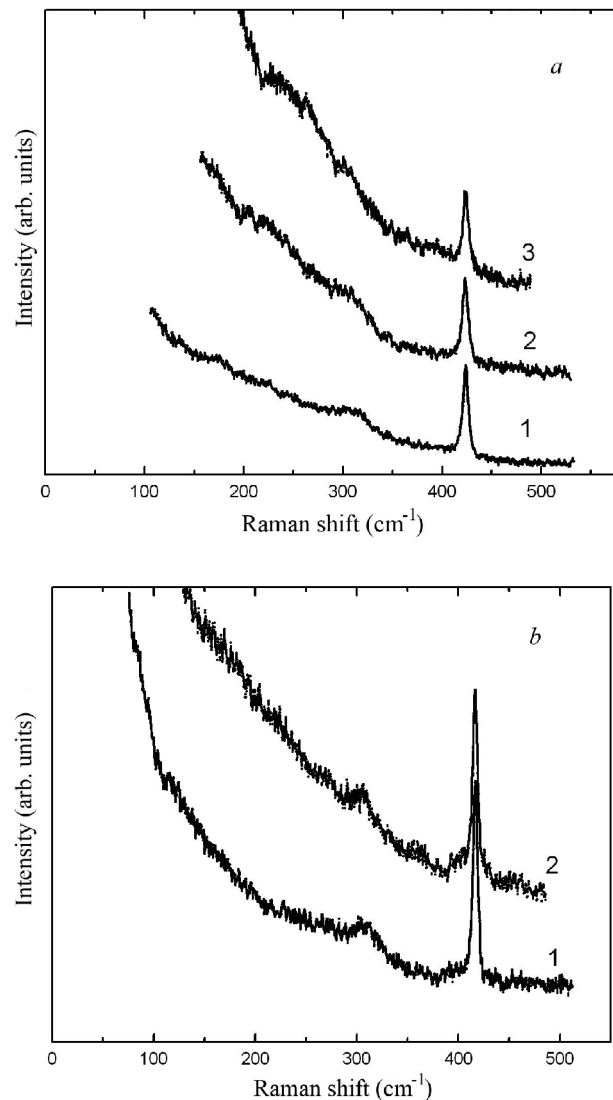
Fig. 1. SEM image for a nanocomposite with CSMA based on Cu_6PS_5Br with the average grain size 38 nm (the concentration of nanocrystals is 1/3 of the sample weight).
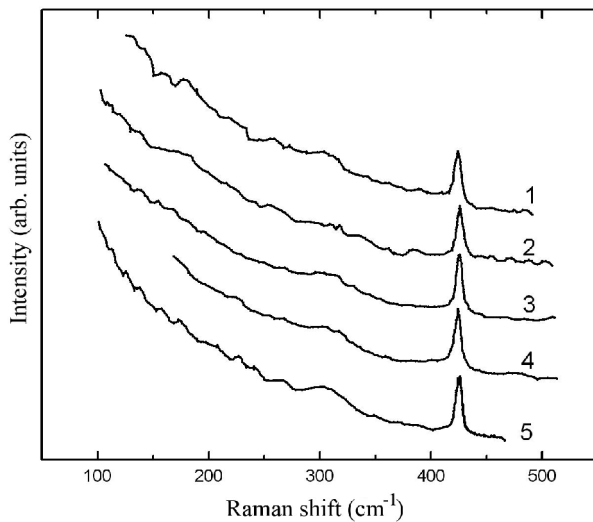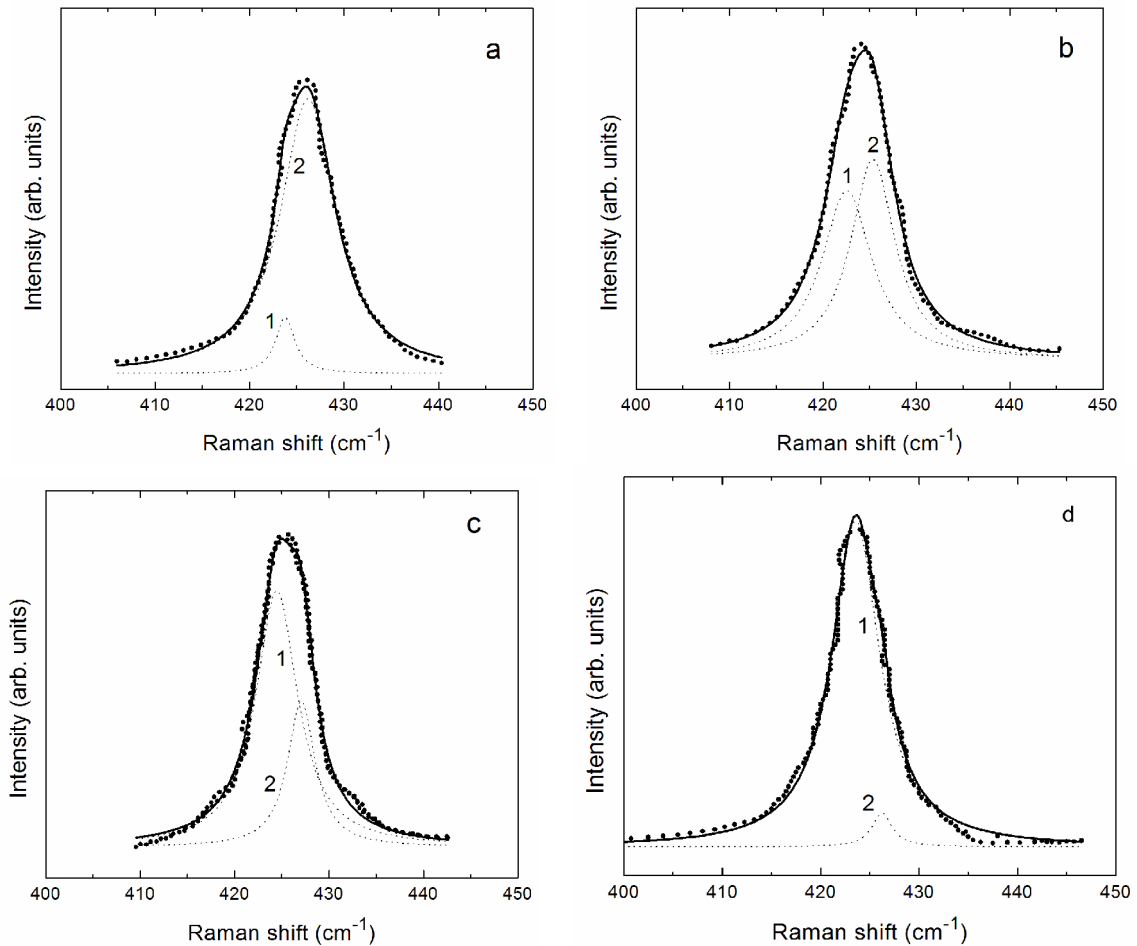

Fig. 2. Raman spectra of the nanocomposite with PFE (*1*), with PVC (*2*), with CSMA (*3*), with CSMA and plastificator (dibutylphtalate) (*4*), as well as with CSMA and a stabilizing agent (trys-(hydroxymethyl) methylamine) (*5*), based on Cu_6PS_5Br with the average grain size 38 nm (the concentration of the nanocrystals is 1/3 of the sample weight).

It should be noted that in nanometric crystals the low-frequency shift of Raman bands and their broadening are most often explained by confinement-related selection rules violation due to the small crystal size [15] and surface phonon modes [16]. In our case, the former factor seems to be hardly possible, because the minimal nanocrystal size studied here (15 nm) is, according to the calculations in [17], too big to ascribe the observed features of the size-related behaviour of the Raman band parameters to the phonon confinement. As an alternative, the observed changes in the Raman spectra of nanocomposites can be assigned to Fröhlich surface phonon modes.

One should note that the A_1 mode is a fully symmetrical vibration for the case of an ideal free PS_4 tetrahedron. However, due to the crystal field this vibration becomes slightly polar, and the polarity increases with the size decrease due to the breakdown and changes of the chemical bonds for the tetrahedra directly at the nanocrystal surface. Therefore, the explanation of the observed shift and broadening the Raman features with the average size reduction by the increasing contribution of the surface phonon scattering is quite reasonable.

Fig. 3. Raman spectra of nanocomposite with CSMA based on Cu_6PS_5Br (*a*) and Cu_6PS_5I (*b*) nanocrystals with different average grain sizes and concentration: (*1a*): *d* = 38 nm, concentration is 2/3 of the sample weight; (*2a*): *d* = 15 nm, concentration is 2/3 of the sample weight; (*3a*): *d* = 15 nm, concentration is 1/3 of the sample weight; (*1b*): *d* = 93 nm, concentration is 2/3 of the sample weight; (*2b*): *d* = 35 nm, concentration is 2/3 of the sample weight.

Fig. 4. Part of the Raman spectrum including the most intense A_1 band for the nanocomposite with PVC (*a*), the nanocomposite with PFE (*b*), the nanocomposite with CSMA (*c* – the concentration of the nanocrystals is 1/3 of the sample weight) and the nanocomposite with CSMA (*d* – the concentration of the nanocrystals is 2/3 of the sample weight) based on Cu_6PS_5Br with the average grain size 38 nm and its simulation by two Lorentzian contours corresponding to surface (*1*) and "bulk" (*2*) phonons, which frequencies and halfwidths are given in Table 1.

In order to estimate the contribution of surface phonon modes to the experimentally measured spectra, we have approximated the A_1 Raman band by a superposition of two Lorentzian contours, the results being shown in Figs 4 and 5. It is clearly seen from Tables 1 and 2 that the A_1 band is well fitted by two peaks, the lower-frequency peak mainly being broader than the higher-frequency one. First, it is shown that in comparison with nanopowders introduction of nanocrystals into the polymer matrices leads to an increase of the frequencies of the "bulk" and surface phonons, while their halfwidths depend on the type of the polymer (Tables 1 and 2). Besides, an increase of the concentration of nanocrystals and a decrease of their average grain size cause a decrease of the "bulk" phonons halfwidth and an increase of the surface phonon halfwidth. Finally, the surface-to-bulk phonon integrated intensity ratio (SBPIIR) strongly varies with the type of the polymer matrix, average grain size and concentration of nanocrystals. Thus, the greatest SBPIIR among the polymer matrices is observed for CSMA (Fig. 4). It means that the above mentioned polymer is promising material to form nanocomposites, because the number of separate nanocrystals is higher than in other polymer matrices, in which the nanocrystals are conglomerated. Introduction of a plastificator and stabilizing agent improves mechanical properties of nanocomposites but leads to a decrease of SBPIIR. The increase of the concentration of nanocrystals and the decrease of their average grain size determine the increase of SBPIIR (Figs 4 and 5).

Table 1. Spectral positions and halfwidths of "bulk" and surface phonons in nanocomposites based on Cu_6PS_5Br.

Material	"bulk" phonon		surface phonon	
	ω (cm^{-1})	Γ (cm^{-1})	ω (cm^{-1})	Γ (cm^{-1})
Nanocrystalline powders (grain size – 38 nm)	423	6.7	421	7.7
Nanocomposite with PVC	427	7.0	424	4.3
Nanocomposite with PFE	426	5.8	423	6.5
Nanocomposite with CSMA (the concentration of the nanocrystals is 1/3 of the sample weight)	427	3.6	425	5.4
Nanocomposite with CSMA and plastificator (dibutylphtalate)	425	5.5	421	7.4
Nanocomposite with CSMA and stabilizing agent (trys-(hydroxymethyl) methylamine)	427	4.2	424	5.8
Nanocomposite with CSMA (the concentration of the nanocrystals is 2/3 of the sample weight)	426	2.5	424	5.9

Table 2. Spectral positions and halfwidths of "bulk" and surface phonons in nanocomposites based on Cu_6PS_5I.

| Material	"bulk" phonon		surface phonon	
	ω (cm^{-1})	Γ (cm^{-1})	ω (cm^{-1})	Γ (cm^{-1})
Nanocrystalline powders (grain size – 35 nm)	417	5.3	414	8.5
Nanocomposite with CSMA and crystals of 93 nm (the concentration of the nanocrystals is 2/3 of the sample weight)	418	4.6	415	4.7
Nanocomposite with CSMA and crystals of 35 nm (the concentration of the nanocrystals is 2/3 of the sample weight)	418	1.0	416	6.1

4. Conclusions

Cu_6PS_5X (X = I, Br) nanocrystals were obtained by ball milling, their average size was estimated from X-ray diffraction measurements. Nanocomposites were obtained by mixing with solution of different polymers, plastificators and stabilizing agents. Structural studies by scanning electron microscopy have shown that part of nanocrystals are uniformly distributed in the polymer matrix, while the rest of them are conglomerated in rather large units that are more by an order of magnitude higher than the average grain size.

In polymer nanocomposites, an essential growth of Rayleigh scattering is observed, the Raman spectra contain only the A_1 band, while the one formed by the superposition of E and F_2 symmetry modes, is either pronounced very weakly, or not revealed at all. The evolution of the Raman spectra is explained predominantly by surface phonon modes, which contribution to the Raman spectrum increases due to the higher surface-to-volume ratio.

Contribution of surface phonon modes to the experimentally measured Raman band was estimated. Embedding the nanocrystals into polymer matrices leads to an increase of frequencies of the "bulk" and surface phonons, while their halfwidths depend on the type of the polymer. The surface-to-bulk phonon integrated intensity ratio strongly varies with the type of the polymer matrix, average grain size and concentration of nanocrystals. It is shown that CSMA is promising material as a polymer matrix to form nanocomposites. The increase of the concentration of nanocrystals and decrease of their average grain size determine the increase of surface-to-bulk phonon integrated intensity ratio.
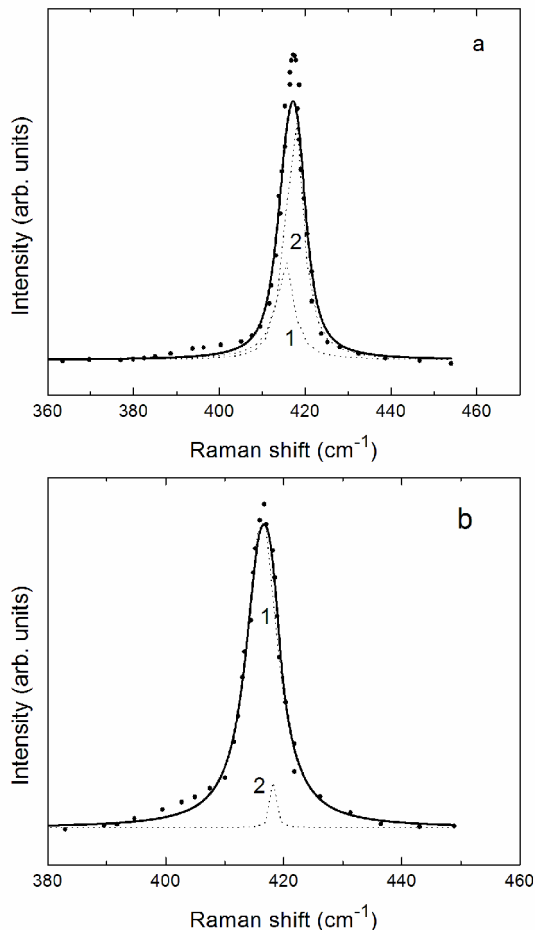
Fig. 5. Part of the Raman spectrum including the most intense A_1 band for the nanocomposite with CSMA based on Cu_6PS_5I (the concentration of the nanocrystals is 2/3 of the sample weight) with the average grain size 93 (*a*) and 35 nm (*b*) as well as its simulation by two Lorentzian contours corresponding to surface (*1*) and "bulk" (*2*) phonons, which frequencies and halfwidths are given in Table 2.

References

1. W.F. Kuhs, R. Nitsche, K. Scheunemann, Vapour growth and lattice data of new compounds with icosahedral structure of the type Cu_6PS_5Hal (Hal = Cl, Br, I) // *Mater. Res. Bull.* **11**, p. 1115-1124 (1976).
3. T. Nilges, A. Pfitzner, A structural differentiation of quaternary copper argirodites: Structure – property relations of high temperature ion conductors // *Z. Kristallogr.* **220**, p. 281-294 (2005).
3. R.B. Beeken, J.J. Garbe, N.R. Petersen, Cation mobility in the Cu_6PS_5X (X = Cl, Br, I) argyrodites // *J. Phys. Chem. Solids*, **64**, p. 1261-1264 (2003).
4. I.P. Studenyak, V.O. Stefanovich, M. Kranjčec, Yu, M. Azhnyuk, Gy.Sh. Kovacs, V.V. Panko, Raman scattering studies of Cu_6PS_5Hal (Hal = Cl, Br, I) fast-ion conductors // *Solid State Ionics*, **95**, p. 221-225 (1997).
5. A. Gagor, A. Pietraszko, D. Kaynts, Diffusion paths formation for Cu ions in superionic Cu_6PS_5I single crystals studied in terms of structural phase transition // *J. Solid State Chem.* **178**, p. 3366-3375 (2005).
6. A. Haznar, A. Pietraszko, I.P. Studenyak, X-ray study of the superionic phase transition in Cu_6PS_5Br // *Solid State Ionics*, **119**, p. 31-36 (1999).
7. S. Fiechter, E. Gmelin, Thermochemical data of argyrodite-type ionic conductors: Cu_6PS_5Hal (Hal = Cl, Br, I) // *Thermochim. Acta*, **85**, p. 155-158 (1985).
8. V. Samulionis, J. Banys, Y. Vysochanskii, I. Studenyak, Investigation of ultrasonic and acousto-electric properties of ferroelectric-semiconductor crystals // *Ferroelectrics*, **336**, p. 29-38 (2006).
9. I.P. Studenyak, M. Kranjčec, Gy.S. Kovacs, V.V. Panko, I.D. Desnica, A.G. Slivka, P.P. Guranich, The effect of temperature and pressure on the optical absorption edge in Cu_6PS_5X (X = Cl, Br, I) crystals // *J. Phys. Chem. Solids*, **60**, p. 1897-1904 (1999).
10. A.F. Orliukas, E. Kazakevicius, A. Kezionis, T. Salkus, I.P. Studenyak, R.Yu. Buchuk, I.P. Prits, V.V. Panko, Preparation, electric conductivity and dielectrical properties of Cu_6PS_5I-based superionic composites // *Solid State Ionics*, **180**, p. 183-186 (2009).
11. I.P. Studenyak, R.Yu. Buchuk, M. Kranjčec, I.I. Makauz, I.M. Voynarovych, L. Daroczi, I. Charnovich, S. Kökényesi, Structural, electrical, and optical properties of As_2S_3-Cu_6PS_5I nanocomposites // *J. Non-Cryst. Solids*, **357**, p. 96-99 (2011).
12. I.P. Studenyak, R.Yu. Buchuk, V.O. Stephanovich, S. Kökényesi, M. Kis-Varga, Luminescent properties of Cu_6PS_5I nanosized superionic conductors // *Radiation Measurements*, **42**, p. 788-791 (2007).
13. M. Kranjčec, I.P. Studenyak, R.Yu. Buchuk, V.O. Stephanovich, S. Kökényesi, M. Kis-Varga, Structural properties and Raman scattering in Cu_6PS_5X (X = I, Br) nanocrystalline solid electrolytes // *Solid State Ionics*, **179**, p. 218-221 (2008).
14. I.P. Studenyak, R.Yu. Buchuk, M. Kranjčec, V.O. Stephanovich, V.V. Panko, S. Kokenyesi, Peculiarities of Raman scattering in nanometric Cu_6PS_5Br superionic conductors // *Ukr. J. Phys. Opt.* **10**, p. 150-156 (2009).
15. A. Ingale, K.C. Rustagi, Raman spectra of semiconductor nanoparticles: Disorder-activated phonons // *Phys. Rev. B*, **58**, p. 7197-7204 (1998).
16. Y.N. Hwang, S.H. Park, D. Kim, Size-dependent surface phonon mode of CdSe quantum dots // *Phys. Rev. B*, **59**, p. 7285-7288 (1998).
17. A.V. Gomonnai, I.M. Voynarovych, A.M. Solomon, Yu.M. Azhniuk, A.A. Kikineshi, V.P. Pinzenik, M. Kis-Varga, L. Daroczy, V.V. Lopushansky, X-ray diffraction and Raman scattering in SbSI nanocrystals // *Mat. Res. Bull.* **38**, p. 1767-1772 (2003).